Molecular Mechanisms Involved in Lymphocyte Recruitment in Inflamed Brain Microvessels: Critical Roles for P-Selectin Glycoprotein Ligand-1 and Heterotrimeric G ¡-Linked Receptors

Laura Piccio, Barbara Rossi, Elio Scarpini, Carlo Laudanna, Cinzia Giagulli, Andrew C. Issekutz, Dietmar Vestweber, Eugene C. Butcher and Gabriela Constantin

J Immunol 2002; 168:1940-1949; ;
doi: 10.4049/jimmunol.168.4.1940
http://www.jimmunol.org/content/168/4/1940

The Journal of Immunology is published twice each month by
The American Association of Immunologists, Inc.,
1451 Rockville Pike, Suite 650, Rockville, MD 20852

Print ISSN: 0022-1767 Online ISSN: 1550-6606.

Molecular Mechanisms Involved in Lymphocyte Recruitment in Inflamed Brain Microvessels: Critical Roles for P-Selectin Glycoprotein Ligand-1 and Heterotrimeric G_i-Linked Receptors[1]

Laura Piccio,*† Barbara Rossi,* Elio Scarpini,† Carlo Laudanna,* Cinzia Giagulli,* Andrew C. Issekutz,‡ Dietmar Vestweber,§ Eugene C. Butcher,¶ and Gabriela Constantin[2]*

Lymphocyte recruitment into the brain is a critical event in the pathogenesis of multiple sclerosis and experimental autoimmune encephalomyelitis. We developed a novel intravital microscopy model to directly analyze through the skull the interactions between lymphocytes and the endothelium in cerebral venules of mice. No adhesive interactions were observed between lymphocytes and the nonactivated endothelium in the cerebral microcirculation. When brain venules were activated by pretreating mice with TNF-α or LPS, proteolipid protein 139–151 autoreactive T lymphocytes rolled and arrested; notably, only a few peripheral lymph node cells rolled and firmly adhered. Abs anti-P-selectin glycoprotein ligand-1 and anti-E- and P-selectin blocked tethering and rolling of autoreactive lymphocytes, suggesting that P-selectin glycoprotein ligand-1/endothelial selectins are critical in the recruitment of lymphocytes in inflamed brain venules. E- and P-selectin were expressed on cerebral vessels upon in vivo activation and had a patchy distribution during the preclinical phase of active and passive experimental autoimmune encephalomyelitis. LFA-1/ICAM-1 and α_4 integrins/VCAM-1 supported rolling, but were not relevant to rolling velocity. Firm arrest was mainly mediated by LFA-1 and ICAM-1. Pretreatment of autoreactive lymphocytes with pertussis toxin blocked integrin-dependent arrest, implicating a requirement for G_i protein-dependent signaling in vessels from nonlymphoid districts. In conclusion, our data unveils the molecular mechanisms controlling the recruitment of autoreactive lymphocytes in inflamed cerebral vessels and suggest new insights into the pathogenesis of autoimmune inflammatory diseases of the CNS. ***The Journal of Immunology,*** **2002, 168: 1940–1949.**

Multiple sclerosis (MS)[3] and its animal model, experimental autoimmune encephalomyelitis (EAE), are inflammatory autoimmune diseases of the CNS mediated by lymphocytes reactive to brain Ags (1, 2). Two possibilities regarding the initiation of inflammation in MS have been considered (3). The first is that autoreactive $CD4^+$ T cells, as shown in EAE, enter the normal brain parenchyma and initiate an autoimmune response against brain Ags. The second possibility is that virus Ag-specific T cells cross into the brain and target virally infected CNS-resident APC, as shown in virus-induced encephalitis (4). From both these possibilities, it clearly emerges that the emigration of autoreactive lymphocytes through the blood-brain barrier (BBB) represents a critical pathogenetic event in the initiation of CNS inflammation.

The process leading to lymphocyte extravasation is a finely regulated sequence of steps controlled by both adhesion molecules and activating factors. It involves: 1) initial contact (tethering or capture) and rolling along the vessel wall mediated by selectins and integrins, and their ligands; 2) chemoattractant-induced heterotrimeric G_i protein-dependent intracellular biochemical changes leading to integrin activation; 3) integrin-dependent firm arrest; and 4) diapedesis (5–7). Although this sequence of events likely represents a stereotyped leukocyte response to proadhesive and chemotactic stimuli, selective recruitment of various lymphocyte subtypes under physiological and pathological situations depends on the action of different classes of adhesion molecules and activating factors whose combination generates a tissue-specific "area code" (8). Previous immunohistologic studies have shown that resting lymphocytes do not breach the BBB. In contrast, activated T lymphocytes, can cross the BBB regardless of their Ag specificity, but only T cells that recognize the CNS Ag persist and can recruit other inflammatory cells (9). Therefore, it is believed that the state of activation of lymphocytes is more important in inflammatory cell homing to the brain than Ag specificity (10). In vitro adhesion assays have shown that binding of lymphocytes to inflamed brain vessels is mainly mediated by LFA-1/ICAM-1, very

*Department of Pathology, University of Verona, Verona, Italy; †Department of Neurological Sciences, Istituto di Ricovero e Cura a Carattere Scientifico, Ospedale Maggiore Policlinico, and "Dino Ferrari" Center, Milan, Italy; ‡Department of Pediatrics, Pathology, and Microbiology-Immunology, Dalhousie University, Halifax, Nova Scotia, Canada; §Institute of Cell Biology, Center for Molecular Biology of Inflammation, University of Muenster, and Max-Planck-Institut, Muenster, Germany; and ¶Department of Pathology, Stanford University, Stanford, CA 94305

Received for publication September 6, 2001. Accepted for publication December 5, 2001.

The costs of publication of this article were defrayed in part by the payment of page charges. This article must therefore be hereby marked *advertisement* in accordance with 18 U.S.C. Section 1734 solely to indicate this fact.

[1] This work was supported by Istituto Superiore di Sanità, Ministero dell'Università e della Ricerca Scientificae Tecnologica, Fondazione Italiana Sclerosi Multipla (2000/R/71), Ministero della Sanità ("ricerca finalizzata"), and Consiglio Nazionale delle Ricerche (00.00154. ST74) (to G.C.); Associazione "Amici del Centro Dino Ferrrari" and Istituto di Ricovero e Cura a Carattere Scientifico Ospedale Maggiore Policlinico, Milano, Italy (to E.S.); Associazione Italiana Ricerca sul Cancro (to C.L.), and the Deutsche Forschungsgemeinschaft, Sonderforschungsbereich 293 (to D.V.). B.R. was supported by funds from Research and Innovation, Padova, Italy.

[2] Address correspondence and reprint requests to Dr. Gabriela Constantin, Department of Pathology, Section of General Pathology, University of Verona, Strada le Grazie 8, Verona 37134, Italy. E-mail address: gabriela.constantin@univr.it

[3] Abbreviations used in this paper: MS, multiple sclerosis; EAE, experimental autoimmune encephalomyelitis; BBB, blood-brain barrier; VLA, very late activation Ag; PSGL, P-selectin glycoprotein ligand; PTX, pertussis toxin; PLN, peripheral lymph nodes; PLP, proteolipid protein.

0022-1767/02/$02.00

late activation antigen (VLA)-4/VCAM-1 (11, 12). Moreover, blocking Abs against adhesion molecules involved in the interactions between leukocytes and endothelium are able to inhibit the development of EAE, suggesting that interfering with not yet well elucidated steps of leukocyte extravasation can be therapeutic for autoimmune inflammatory diseases of the brain (12–15). It was previously shown that anti-P-selectin Abs are able to block leukocyte rolling on nicotine-activated endothelium in pial vessels (16). Recent intravital microscopy work has shown that both E- and P-selectin are required for efficient tethering and rolling of neutrophils in brain vessels in mice treated with TNF-α (17). Moreover, a recent immunohistologic study suggested that P-selectin may be involved in the early recruitment of encephalitogenic lymphocytes into the brain (18).

All intravital microscopy studies used until now to determine the interactions between blood-circulating leukocytes and brain endothelium were conducted by performing a cranial window into the skull using a drill. In these experiments, animals need to be artificially ventilated, while bleeding and tissue overheating from cautery may occur. So far, no study has been performed to determine the behavior of different leukocyte subpopulations and of cells in different states of activation in cerebral vessels. The present study was designed to assess the adhesion cascade of lymphocytes in brain microcirculation. We set up a novel intravital microscopy model allowing visualization of cerebral vessels through the skull and analysis of the interactions between different lymphocyte subpopulations and the endothelium in the brain microvasculature of mice. Our findings show that brain endothelium in EAE-susceptible mice requires activation to support adhesive events and that activated, but not resting, lymphocytes interact efficiently. We also provide evidence that P-selectin glycoprotein ligand-1 (PSGL-1) and endothelial selectins represent key molecules in the recruitment of lymphocytes into the brain. E- and P-selectin are expressed during preclinical EAE suggesting a role for these molecules in the recruitment of leukocytes in the pathology of brain inflammation. Moreover, we show that LFA-1 and ICAM are critical in lymphocyte adhesion and that integrin-dependent arrest requires heterotrimeric G_i protein-dependent signaling. We conclude that the brain endothelium expresses a combination of adhesion ligands and activating factor(s) for G_i-linked receptors that together mediate lymphocyte recruitment, and that the combination of molecules involved in this CNS venule-adhesion cascade strongly favors the arrest of activated vs naive T cells.

Materials and Methods

Reagents

Anti-L-selectin Mel-14, anti-α_4 PS/2, anti-LFA-1 α-chain TIB213, anti-VCAM-1 MK 2.7, and anti-ICAM-1 YN 1.1.7.4 mAbs were obtained from American Type Culture Collection (Manassas, VA). Anti-E- and P-selectin (anti-E-selectin and anti-P-selectin) and anti-PSGL-1 (4RA10) Abs were obtained as previously described (19–21). Green 5-chloromethylfluorescein diacetate or orange 5-(and-6)-(((chloromethyl)benzoyl)amino)tetramethylrhodamine (Molecular Probes, Eugene, OR) were prepared as a stock solution in DMSO and kept at −20°C until the moment of use. Pertussis toxin (PTX) was purchased from Calbiochem (Inalco, Italy) and the mutant PTX having two amino acid substitution (PT9K/129G) was a generous gift of Dr. R. Rappuoli (Chiron Biocine, Siena, Italy).

Preparation of lymphocytes and fluorescent labeling

Resting lymphocytes were obtained from peripheral lymph nodes (PLN) from young adult SJL mice. Cell number and viability were assessed by trypan blue exclusion.

Production, characterization, and maintenance of proteolipid protein (PLP) 139–151-specific T cell lines was as previously described (22). In brief, SJL/J mice were immunized with 250 μg of peptide PLP139–151. Ten days later, draining lymph nodes were removed and stimulated with 30 μg/ml peptide for 4 days. T cell lines were obtained by stimulation of these cultures every 14 days with irradiated syngenic spleen cells at a ratio of 1:10 (T cell vs irradiated spleen cells). For the intravital microscopy experiments, lymphocytes were Ag-stimulated for 4 days and then kept for 1–5 days in Ag-free medium. Lymphocytes were starved of Ag after antigenic stimulation to reduce background adhesiveness and to be able to reveal inside-out signaling generated by local proadhesive agonists.

For intravital microscopy experiments, lymphocytes were suspended at a concentration of 0.5×10^6/ml in DMEM without sodium bicarbonate (Sigma-Aldrich, St. Louis, MO), supplemented with 20 mM of HEPES, 5% FCS (pH 7.1) and were labeled with either green 5-chloromethylfluorescein diacetate (Molecular Probes) or orange 5-(and-6)-(((chloromethyl)benzoyl)amino)tetramethylrhodamine (Molecular Probes) for 20 min at 37°C.

Animal preparation for intravital microscopy

SJL young females were purchased from Harlan-Nossan (Udine, Italy) and were housed and used according to current European community rules for the usage of laboratory animals. Mice received no treatment or were injected i.p. with 12 μg of LPS (*Escherichia coli*, 026:B6; Sigma-Aldrich) or i.v. with 1 μg of TNF-α, 5–6 h or 3–4 h, respectively, before starting the intravital experiment. Animals were anesthetized by i.p. injection (10 ml/kg) of physiologic saline containing with ketamine (5 mg/ml) and xylazine (1 mg/ml). The recipient was maintained at 37°C by a stage-mounted strip heater Linkam CO102 (Olympus, Melville, NY). A heparinized PE-10 polyethylene catheter was inserted into the right common carotid artery toward the brain. To exclude the noncerebral vessels from the analysis, the right external carotid artery and the pterygopalatine artery, a branch from the internal carotid, were ligated. The scalp was reflected, the skull was bathed with sterile saline, and a 24 mm × 24 mm coverslip was applied and fixed with silicon grease. A round chamber with an 11-mm internal diameter was attached onto the coverslip and filled with water.

Intravital videomicroscopy

The preparation was placed on an Olympus BX50WI microscope and a water immersion objective with long focal distance (Olympus Achroplan, focal distance 3.3 mm, NA 0.5 ∞) was used. Blood vessels were visualized by using fluorescent dextrans: 3 mg of FITC-dextran (148 kDa; Sigma-Aldrich) and/or 6 mg of tetramethylrhodamine isothiocyanate-dextran (155kDa; Sigma-Aldrich) were diluted in 0.3 ml of sterile physiologic saline and centrifuged for 5 min at 14,000 × *g* (each mouse received 0.05 ml of supernatant). Fluorescent-labeled cells (2.5×10^6)/condition were slowly injected into the carotid artery by a digital pump at a flow rate of 0.13–1 μl/s. The images were visualized by using a silicon-intensified target videocamera (VE-1000 SIT; Dage-MTI, Michigan, IL) and a Sony SSM-125CE monitor (Tokyo, Japan). Recordings were digitalized and stored on videotapes using a digital VCR (Panasonic NV-DV10000; Secaucus, NJ) and Casablanca digital system (MS MacroSystem Computer, Witten, Germany). The recordings were made during the injection of the cells and for a few minutes after the injection ended.

Image analysis

Video analysis was performed by playback of digital videotapes in real time, or at reduced speed, and frame by frame. Vessel diameter (D), hemodynamic parameters, and the velocities of rolling were determined by using a PC-based system including a LG-3 frame grabber (Psion Corporation, Frederick, MD), NIH Image software 1.61, and a Casablanca digital system (MS MacroSystem Computer). The velocities of ≥20 consecutive freely flowing cells/venule were calculated and from the velocity of the fastest cell in each venule (V_{fast}), we calculated the mean blood flow velocities (V_m): $V_m = V_{fast}/(2 - \epsilon^2)$, where ϵ is the ratio of the lymphocyte diameter to the vessel diameter (23). The wall shear rate (γ) was calculated from $\gamma = 8 \times V_m/D$ (s^{-1}) and the shear stress (τ) acting on rolling cells was approximated by $\gamma \times 0.025$ (dyne/cm^2), assuming a blood viscosity of 0.025 poise. Lymphocytes were considered as rolling if they traveled at velocities below V_{crit} ($V_{crit} = V_m \times \epsilon \times (2 - \epsilon)$) (23). Lymphocytes that remained stationary on the venular wall for ≥30 s were considered adherent. At least 140 consecutive cells/venule were examined. Rolling and firm arrest fractions were determined as the percentage of cells that rolled or firmly arrested within a given venule in the total number of cells that enter that venule during the same period (24).

In vivo staining of endothelial adhesion molecules

Anti-E- and P-selectin, anti-VCAM-1, and anti-ICAM-1 mAbs and an isotype-matched control Ab (anti-human Ras) were labeled using an Alexa Fluor 488 labeling kit (Molecular Probes). For some experiments, control mAb was also labeled using an Alexa Fluor 566 kit. Fifty micrograms of fluorescent mAb were injected i.v. Twenty minutes later, the animal was anesthetized and perfused through the left ventricle and through a catheter

inserted into the right carotid with cold PBS. The skull and meninges were removed and cerebral vessels were visualized using the intravital microscopy setting.

Induction of active and passive EAE

Six- to 8-wk-old SJL/J females were purchased from Harlan-Nossan. PLP139-151-specific T cell lines were produced as previously described (22). Ag-stimulated T cells (25×10^6) were injected i.v. into mice. In the case of active EAE induction, mice were immunized s.c. with 300 μg of PLP139–151 as previously described (25). Mice were checked daily and scored for EAE (22, 25).

Statistics

Statistical analysis of the results was performed by using SPSS 10.0 software (SPSS, Chicago, IL). A two-tailed Student's *t* test was used for statistical comparison of two samples. Multiple comparisons were performed using the Kruskall-Wallis test with the Bonferroni correction of *P*. Velocity histograms were compared using the Mann-Whitney *U* test and the Kolmogorov-Smirnov test. Linear regressions were analyzed using the Spearman rank correlation test. Differences were regarded significant with a value of $p < 0.05$.

Results

Visualization of cerebral superficial vessels

The parietal skull was sufficiently transparent to allow for the observation of superficial cerebral vessels. To exclude the bone vessels, bone marrow vessels, and meningeal vessels from our analysis, we ligated both the right external carotid and the right pterygopalatine artery (Fig. 1*A*). The pterygopalatine artery is an extracranial branch of the internal carotid and it vascularizes mostly extracranial structures, with the notable exception of the middle meningeal artery, a branch we needed to exclude because the analysis was performed in parietal vessels (26). Arterioles were identified as vessels with divergent bifurcations, whereas confluent branches defined venular segments (23). Many of the branches of superficial cerebral venules have a characteristic "interrupted" shape with convex origins which are due to their emergence on the brain surface from the more profound layers (Fig. 1*B*). This peculiarity of cerebral veins makes them easily recognizable and clearly distinguishes them from bone and meningeal vessels. We compared the hemodynamic characteristics of right and left main cerebral veins and no significant differences were observed during the time course of our experiments (not shown). The analysis of the injected fluorescent cells could be performed in cerebral vessels of the ipsilateral hemisphere of the brain after carotid ligation, but also in the contralateral hemisphere where cells arrive through the circle of Willis.

Nonactivated brain endothelium does not support lymphocyte interactions

Two populations of lymphocytes were used to study the interactions with nonactivated brain endothelium: resting cells freshly isolated from PLN cells and autoreactive T cells specific for PLP139–151 (Table I; data not shown). The behavior of autoreactive T cells was studied in 30 venules with diameters ranging from 18 to 104 μm in 9 animals. Similar experiments were performed with PLN cells (data not shown). Fluorescently labeled lymphocytes were slowly injected by using a digital pump. In each venule, at least 140 consecutive cells were examined. Neither of the two lymphocyte populations rolled or firmly adhered to normal brain endothelium (Table I; data not shown). Some autoreactive lymphocytes were mechanically entrapped in capillaries, but this caused no significant modification of the hemodynamic parameters. We concluded that nonactivated brain endothelium does not support lymphocyte interactions.

We next performed some additional controls to test the sensitivity of our new intravital microscopy method and to study the adhesive interactions between autoreactive lymphocytes and the endothelium in brain vessels vs noncerebral vessels. When both pterygopalatine and external carotid arteries were not ligated, the cells flowed into the bone marrow, skull, and meningeal vessels. Some adhesive interactions were observed in bone marrow vessels. However, the number of cells we visualized was very low. When we ligated only the external carotid artery, autoreactive lymphocytes flowed into bone marrow vessels, some meningeal vessels under the parietal bone, and cerebral vessels. Rolling and firm arrest occurred only in bone marrow vessels. The percentage of rolling cells in bone marrow vessels was 2.5 ± 2.4% (mean ± SD) while the percentage of cells that arrested was 2.1 ± 1.5% (mean ± SD; data not shown). These results are supported by previous data showing that bone marrow vessels constitutively express E- and P-selectin and VCAM-1 (27). Noninflamed cerebral and meningeal vessels did not support rolling or arrest of autoreactive lymphocytes (data not shown).

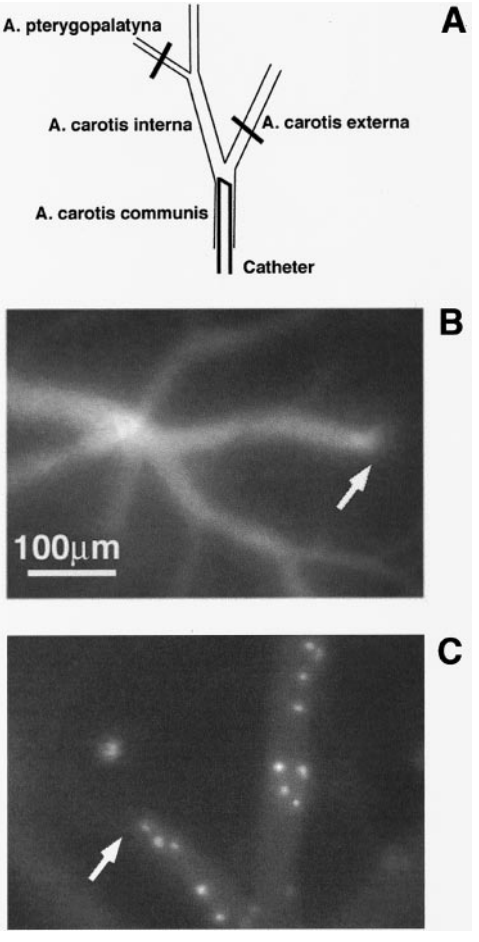

FIGURE 1. Microsurgery and visualization of brain vessels. *A*, A catheter was inserted into the right common carotid artery for the injection of fluorescent cells. To visualize the cells only in cerebral vessels and to exclude the noncerebral vessels, the right external carotid and right pterygopalatine artery were ligated (*B*). Cerebral vessels were visualized by using fluorescent dextrans. Branches of superficial cerebral venules are easily recognizable by their convex origin due to the emergence on the brain surface from the more profound layers (arrow). *C*, A micrograph showing fluorescently labeled PLP139–151-specific T lymphocytes (bright intravascular dots) arrested in inflamed brain venules. Mice were treated with LPS 5–6 h before starting the intravital microscopy experiments. Animals received a low dose of fluorescent dextran. Note the interrupted shape of the vessel (arrow).

Table I. *Diameter, hemodynamics, behavior, and rolling velocities in cerebral venules*[a]

	Nontreated Mice	TNF-Treated Mice	LPS-Treated Mice	
	PLP139–151	PLP139–151	PLP139–151	PLN cells
Number of venules/animals	30/9	10/5	64/30	14/5
Diameter (μm)	45.5 ± 38	52.3 ± 16.8	44.6 ± 15.4	55.8 ± 24.8
V_{fast} (μm/s)	5799 ± 1430	3258 ± 895	3648 ± 1218	3954 ± 1119
V_m (μm/s)	2783 ± 693	1656 ± 356	1302 ± 435	2010 ± 538
WSS (dyne/cm^2)	14.2 ± 3.8	6.4 ± 4.3	5.9 ± 1.9	7.1 ± 2.3
% Rolling	0	6.4 ± 5.9	8 ± 3.7	1.2 ± 1.2
% Firm arrest	0	3.8 ± 3.4	4.5 ± 2.8	0.33 ± 0.31
V_{roll} (μm/s)	0	6.4	5.1	137.4

[a] Mice received no treatment or were treated with TNF-α (1 μg) or LPS (12 μg). Venules were analyzed by individual velocity measurement of at least 20 consecutive noninteracting PLN cells or PLP139–151 autoreactive T cells in each venule. The velocity of the fastest cell in the sample (V_{fast}) was used to determine the mean blood flow velocity (V_m). Venular wall shear rate and wall shear stress (WSS) and the percentages of rolling and arrested cells were calculated as described in *Materials and Methods*. The velocity of 10 rolling cells per venule was measured by digital frame-by-frame analysis of videotapes. V_{roll} are presented as the median. Data are arithmetic mean ± SD.

Behavior of lymphocytes in activated brain venules

It was previously shown that LPS or TNF treatment is able to up-regulate adhesion molecules on the endothelium in vivo (28–30). We next treated the mice with LPS or TNF 5–6 or 3–4 h, respectively, before starting the experiments. Fluorescently labeled lymphocytes were able to roll and arrest (Fig. 1*C*) in inflamed brain venules. The rolling fraction of PLP139–151-specific T cells was significantly higher than for PLN cells (mean ± SD of 8.09 ± 3.78% vs 1.24 ± 1.20%; $p < 0.01$), showing that the activation of lymphocytes increases the frequency of interactions with the brain endothelium (Table I; Fig. 2). The percentages of autoreactive lymphocytes that rolled in mice treated with LPS or TNF were similar (Table I). Rolling fractions inversely correlated with venule diameter but were independent of mean blood flow velocity and wall shear stress (Fig. 3).

We analyzed the quality and strength of rolling by measuring the rolling velocities of resting and autoreactive lymphocytes (Table I; Fig. 4). In mice pretreated with LPS, the median rolling velocity for autoreactive lymphocytes was 5.1 μm/s (Table I). In contrast, the median rolling velocity of PLN cells was 137 μm/s and significant reduction in the fraction of rolling cells <50 μm/s was observed when compared with activated lymphocytes ($p < 0.001$). V_{roll} from different experiments were pooled in velocity class and cumulative V_{roll} histograms were plotted to better analyze the rolling differences between PLN cells and Ag-specific T cells. As shown in Fig. 4*B*, 47% of autoreactive T cells have a V_{roll} of <5 μm/s. Considering the pool of cells that have a V_{roll} <10 μm/s, the difference between PLN cells and autoreactive lymphocytes is striking: the percentage of autoreactive cells is 70%, while PLN cells account only for 9% ($p < 0.001$), suggesting different

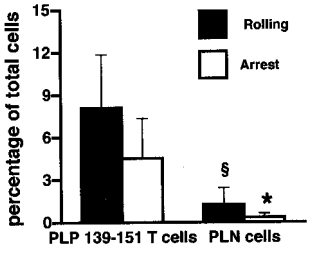

FIGURE 2. Behavior of PLP139–151-specific and resting lymphocytes in brain microcirculation. Mice were treated with 12 μg of LPS 5–6 h before starting the intravital experiments. Resting lymphocytes were freshly isolated from PLNs. PLP139–151-specific lymphocytes were Ag-stimulated for 4 days and then kept for 1–5 days in Ag-free medium before intravital microscopy experiments. Rolling and arrest fractions were calculated. The number of venules or animals for each population is described in Table I. Groups were compared using the Student *t* test. Values of $p <$ 0.001 are for the rolling fraction (§) and arrest fraction (*) of PLN cells when compared with autoreactive lymphocytes. Data shown are mean ± SD.

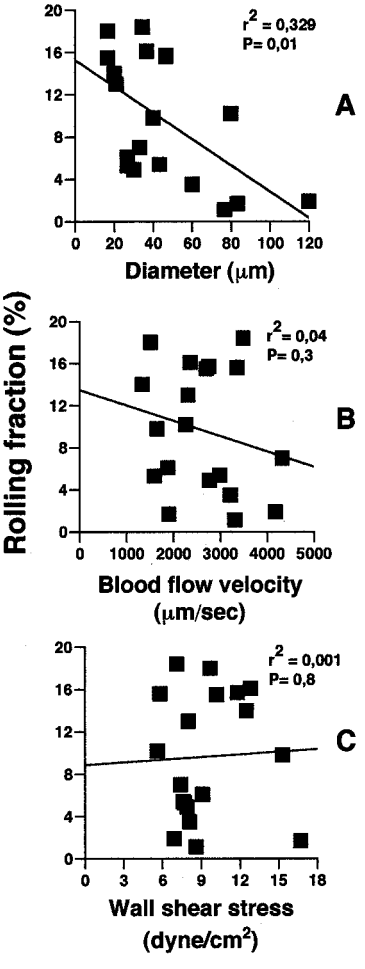

FIGURE 3. Relationship between rolling of brain-specific lymphocytes and microvascular parameters. Each symbol represents the rolling fraction of the L16 autoreactive T cell line in an individual venule of a given diameter. Lymphocytes were Ag-stimulated for 4 days and then kept for 1–5 days in Ag-free medium before intravital microscopy experiments. The number of examined venules was 19. *A*, Regression analysis of autoreactive lymphocyte rolling fractions and vessel diameter indicate a significant inverse correlation ($p = 0.01$). Rolling fractions did not significantly correlate with mean blood flow velocity (*B*) and wall shear stress (*C*) in the same venules.

molecular mechanisms mediating rolling interactions in the two populations. No significant differences in V_{roll} of encephalitogenic lymphocytes was observed between mice treated with LPS and mice treated with TNF (the median, 6.4 μm/s, was obtained by analyzing 69 cells/6 venules/3 mice).

We also analyzed the arrest of lymphocytes in brain vessels. Only a very small percentage of PLN cells firmly adhered to an activated brain endothelium (0.33 ± 0.3) (mean ± SD). In contrast, the mean percentage (±SD) of adherent cells was 4.53 ± 2.83 for encephalitogenic T cells, showing that encephalitogenic lymphocytes adhere significantly more in brain venules than resting cells ($p < 0.001$). As also shown for rolling fractions and V_{roll}, no statistically significant differences were observed between the percentages of firm arrest of autoreactive lymphocytes in mice treated with LPS or TNF. This suggests that the molecular mechanisms controlling the recruitment in cerebral venules in the two experimental models are similar. In conclusion, these results clearly show that autoreactive lymphocytes interact more efficiently than resting cells and represent a more suitable cellular model for further studies.

PSGL-1/endothelial selectins are critical for tethering and rolling of autoreactive lymphocytes

We next endeavored to identify the molecular mechanisms of autoreactive lymphocyte rolling. Lymphocytes were Ag-stimulated for 4 days and then kept for 1–5 days in Ag-free medium before intravital microscopy experiments. Flow cytometry experiments showed a constantly high expression of VLA-4 during the starvation period, whereas LFA-1 and PSGL-1 expression were constantly high between Ag stimulations (data not shown). As we expected, treatment of cells with a mAb to L-selectin had no effect on Ag-activated lymphocyte rolling; in contrast, 96% of tethering and rolling was blocked by an anti-PSGL-1 Ab (Fig. 5*A*). Blocking effects similar to those observed with anti-PSGL-1 Abs were obtained with mAbs to P-selectin and anti-P- and E-selectin used together (inhibition of 96 and 90%, respectively) (Table II and Fig. 5*B*). The anti-E-selectin mAb, when used separately, was also able to substantially block lymphocyte rolling (77% inhibition). These data show that PSGL-1 expression on lymphocytes is critical for capture and rolling and that both E- and P-selectin are required on the endothelium for efficient primary adhesion.

Integrins contribute to rolling, but are not determinants in the strength of rolling

In vivo experiments have shown that integrins and their endothelial ligands may also participate in primary adhesion in vivo (31–33). To determine whether VCAM-1 and α_4 integrins mediate rolling on the activated brain endothelium, we used mAbs against these molecules. Both Abs inhibited rolling fractions by ~50% in

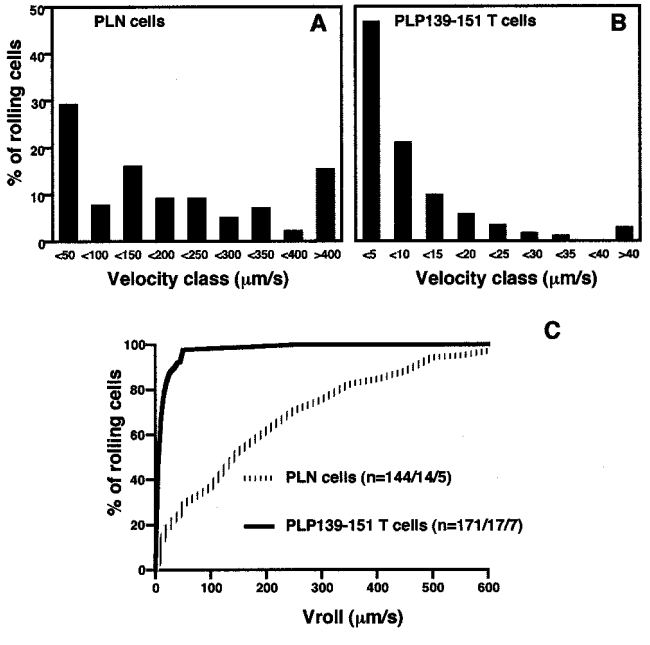

FIGURE 4. Comparison of strength of rolling interactions between PLN cells and PLP139–151-specific T lymphocytes. *A* and *B*, Velocity histograms were generated by measuring rolling velocities as described in *Materials and Methods*. Frequency distributions were calculated after cells were assigned to velocity classes from >0 to 50, 50 to 100, or 100 to 150 μm/s, and so on for PLN cells (*A*), whereas in the case of autoreactive lymphocytes (*B*), cells were assigned to velocity classes from >0 to 5, 5 to 10, or 10 to 15 μm/s, and so on. Lymphocytes were Ag-stimulated for 4 days and then kept for 1–5 days in Ag-free medium before intravital microscopy experiments. *C*, Cumulative velocity curves of PLP139–151 specific T cells and PLN cells. Velocity histograms were compared using the Mann-Whitney *U* test and the Kolmogorov-Smirnov test. Statistical comparison between distribution of cells that had a V_{roll} <50 μm revealed significant differences between the populations ($p < 0.001$); n = the number of cells/venules/mice analyzed.

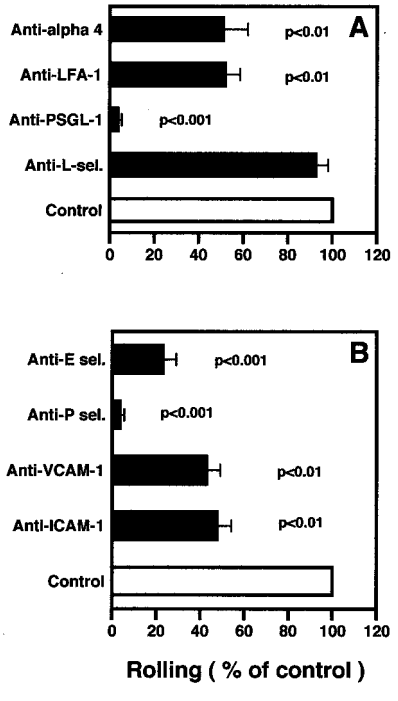

FIGURE 5. Ag-specific T cell rolling in cerebral venules is mainly mediated by PSGL-1. Lymphocytes were Ag-stimulated for 4 days and then kept for 1–5 days in Ag-free medium before intravital microscopy experiments. Rolling fractions were analyzed after treatment of cells and animals with anti-adhesion molecule blocking mAbs expressed by the lymphocytes (*A*) or by the endothelium (*B*). In some experiments (*A*), cells were pretreated with 100 μg/ml mAb for 15 min at 25°C in a total volume of 300 μl and then injected through the right carotid catheter. Then a supplement of up to 100 μg of mAb was administered together with Ab-treated cells. Control cells received no Ab treatment. In other experiments (*B*), mice received 100 μg of mAb before the injection of the cells. Control cells were injected before i.v. mAb administration. Bars depict rolling fractions as a percentage of control cell rolling in the same venule. Data are expressed as mean ± SEM. The number of venules and animals examined for each condition are presented in Table II. Groups were compared with control using the Kruskall-Wallis test followed by Bonferroni correction of *P*.

SJL mice suggesting that $\alpha_4\beta_1$/VCAM-1 are involved in rolling (Fig. 5, *A* and *B*). Furthermore, to a similar extent, anti-LFA-1 and anti-ICAM-1 Abs were also able to inhibit rolling by 48 and 52%, respectively (Fig. 5, *A* and *B*).

It was previously shown in other experimental models that LFA-1 and α_4 integrins are able to strengthen rolling interactions and to reduce rolling velocity (33–35). We asked whether there might be a similarly significant contribution by α_4 and $\alpha_L\beta_1$ integrins to the strength of rolling of PLP139–151 encephalitogenic lymphocytes in brain microcirculation. To address this question, we compared microvascular hemodynamics and V_{roll} (the velocities of at least 10 cells/venule were measured) before and after Ab treatment. No significant effect using the anti-CD11a mAb, anti-α_4 integrins, anti-ICAM-1, and anti-VCAM-1 could be ascertained (Table II).

Firm arrest is mediated by LFA-1-ICAM-1 and α_4 integrin-VCAM-1

To investigate firm arrest, autoreactive lymphocytes were pretreated with an anti-CD11a Ab (TIB213) or with PS/2 mAb anti-α_4 integrins. In other experiments, mice received an anti-ICAM-1 or anti-VCAM-1 mAb. Firm arrest was also examined after the treatment of lymphocytes with the anti-PSGL-1 mAb or after the mice were challenged with anti-E- or P-selectin mAbs. Importantly, sticking was highly blocked by treatment with anti-PSGL-1/endothelial selectins, even when LFA-1 function was not blocked (Fig. 6). Firm arrest was blocked by anti-LFA-1 and anti-ICAM-1 mAbs by 74 and 70%, respectively ($p < 0.001$) (Fig. 6, *A* and *B*). VCAM-1 and α_4 integrins were also involved in firm arrest and anti-VCAM-1 and α_4 integrin Abs blocked ~40% of sticking (Fig. 6, *A* and *B*). These findings suggest that in a subacute model of inflammation, LFA-1/ICAM-1 are central molecules involved in firm arrest in inflamed cerebral vessels.

Activated brain endothelium expresses E- and P-selectin

To determine whether E- and P-selectin are expressed on cerebral vessels after in vivo activation of the endothelium, we injected Alexa 488-labeled anti-E or P-selectin mAbs. Mice received 12 μg of LPS i.p. 5–6 h before the injection of Alexa-labeled mAbs. Twenty minutes after mAb administration, either anti-E- or P-selectin Ab accumulation was detectable with videomicroscopy at the luminal surface of cerebral venules, but not arteries (Fig. 7 and Table III). However, no positivity for anti-selectin mAbs was detected in normal mice (not shown). Alexa 488-labeled anti-ICAM-1 and anti-VCAM-1 Abs accumulated in both arterioles and venules, supporting the data we obtained with blocking Abs. An isotype-matched control Ab revealed no positivity in inflamed cerebral venules (Fig. 7).

Expression of selectins on cerebral vessels during preclinical and clinical phases of EAE

To understand if our intravital microscopy data might be relevant to the pathogenesis of EAE, we next studied the expression of E- and P-selectin during preclinical and clinical phases of both transfer and active EAE. In addition to previous immunohistochemical studies, our videomicroscopy experimental setting allowed us to better explore the expression of selectins on vessels that can be visualized for the majority of their length. Fluorescently labeled Abs were injected in mice and localization to venules was assessed as described above. As shown in Table III, we found venular accumulation of the anti-E-selectin mAb in actively induced EAE on day 5 postimmunization and also during clinical disease (day 9). In transfer EAE, positive vessels for the anti-E-selectin mAb were apparent 2 days postinjection of encephalitogenic cells and E-selectin staining was also detected when disease was clinically evident (day 5; Table III). Previous work suggested a role for P-selectin in the early recruitment of encephalitogenic cells (2 h

Table II. *Venular microhemodynamics, the effect of blocking Abs and PTX, and rolling velocities*[a]

Mice Treatment/mAb		Nr. of Venules/ Animals	Diameter (μm)	V_{fast} (μm/s)	V_m (μm/s)	WSS (dyne/cm^2)	% Rolling	% Firm Arrest	V_{roll} (μm/s)
TNF-treated									
PSGL-1	Control	8/4	50.6 ± 17	3663 ± 706	1852 ± 345	5.7 ± 2.9	6.4 ± 5.9	2.8 ± 3.4	6.8
	mAb	8/4	50.6 ± 17	3246 ± 1884	1637 ± 940	4.65 ± 3.1	0.1 ± 0.01	1.2 ± 0.1	ND
LPS-treated									
L-selectin	Control	6/3	34.9 ± 7	4454 ± 1237	2303 ± 608	13 ± 2.8	4.7 ± 1.6	2.5 ± 0.6	4.4
	mAb	6/3	34.9 ± 7	6014 ± 1766	3042 ± 962	17.4 ± 3.2	4.5 ± 0.7	2.4 ± 0.3	4.3
PSGL-1	Control	8/3	33.5 ± 12.3	4787 ± 1304	2515 ± 616	16.3 ± 5.2	6.7 ± 5	2.1 ± 1.7	7
	mAb	8/3	33.5 ± 12.3	4509 ± 1535	2375 ± 759	15.5 ± 6.9	0.5 ± 0.4	0.4 ± 0.4	ND
E-selectin	Control	6/3	29.8 ± 13.2	4023 ± 1227	2108 ± 637	14.4 ± 4.1	6.3 ± 3.7	7.1 ± 7	4
	mAb	6/3	29.8 ± 13.2	4301 ± 1733	2252 ± 902	15.2 ± 5.8	1 ± 0.4	2.2 ± 1.8	ND
P-selectin	Control	14/6	44.3 ± 10.8	4961 ± 1331	2539 ± 679	11.9 ± 4	6.5 ± 3.1	3.8 ± 2.2	6.9
	mAb	14/6	44.3 ± 10.8	4678 ± 873	2396 ± 450	11.3 ± 3.6	0.2 ± 0.2	0.7 ± 0.6	ND
E- + P-selectin	Control	7/3	36.6 ± 14	3788 ± 1589	1951 ± 804	10.4 ± 2.9	6.4 ± 3.7	1.9 ± 0.9	7.4
	mAb	7/3	36.6 ± 14	4245 ± 470	2189 ± 224	11.9 ± 1.2	0.6 ± 0.4	0.4 ± 0.3	ND
LFA-1	Control	9/4	37.4 ± 10.8	3698 ± 973	1913 ± 500	10.7 ± 3.7	11.8 ± 4.8	7 ± 3.6	7.2
	mAb	9/4	37.4 ± 10.8	4234 ± 912	2191 ± 476	12.4 ± 4.2	6.7 ± 5.6	2 ± 1.8	6.2
ICAM-1	Control	7/4	41 ± 7.7	3897 ± 446	1488 ± 237	7.5 ± 2.3	10.9 ± 4.6	7.1 ± 6.1	4.3
	mAb	7/4	41 ± 7.7	3446 ± 427	1769 ± 220	8.8 ± 2.1	5.5 ± 3.3	2.2 ± 2.1	3.8
α_4-integrins	Control	16/5	53.2 ± 14.8	4946 ± 1230	2518 ± 648	10.3 ± 5.5	7.3 ± 6.5	3.2 ± 2.5	6.6
	mAb	16/5	53.2 ± 14.8	5640 ± 1862	2876 ± 978	12.1 ± 7.5	3.9 ± 3.4	2.2 ± 2	7.6
VCAM-1	Control	6/3	48.6 ± 18	6049 ± 1636	3159 ± 727	13.8 ± 4.3	7.5 ± 4.1	2.3 ± 0.8	7.7
	mAb	6/3	48.6 ± 18	4773 ± 625	2444 ± 277	10.7 ± 3.3	3.8 ± 2.9	1.3 ± 0.3	8
PTX	Control	13/5	52.2 ± 18.7	3973 ± 921	2035 ± 495	9.2 ± 5.5	9.5 ± 3.3	6.2 ± 3.1	7.4
	PTX	13/5	52.2 ± 18.7	3570 ± 923	1826 ± 487	8.1 ± 4.7	12.3 ± 7	1.3 ± 1	7.6

[a] Mice were treated with LPS or TNF 5–6 or 2–3 h, respectively, before starting the intravital microscopy experiment. Treatment with mAbs or PTX was performed as described for Figs. 5, 6, and 9. V_{roll} is presented as the median. Data shown are mean ± SD. ND, not determined.

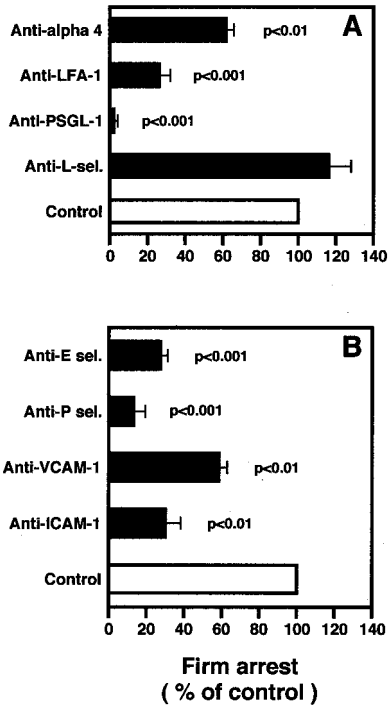

FIGURE 6. Encephalitogenic lymphocyte sticking in cerebral venules is mainly mediated by LFA-1. Lymphocytes were Ag-stimulated for 4 days and then kept for 1–5 days in Ag-free medium before being used for intravital microscopy experiments. Firm arrest fractions were analyzed after treatment of cells and animals with anti-adhesion molecule blocking mAbs expressed by the lymphocytes (*A*) or by the endothelium (*B*). The same experimental protocols and statistical analyses were used as those described for Fig. 5. The fraction of cells that firmly adhered for >30 s was determined before and after treatment of cells or animals with blocking mAbs. Bars represent arrest fractions as a percentage of control cell arrest in the same venule. Data are expressed as mean ± SEM.

postinjection of T cells; Ref. 18). However, we found no anti-P-selectin Ab accumulation in cerebral vessels after 2 h postinjection of encephalitogenic cells (Table III). In active EAE, positivity for anti-P-selectin Abs was detected on day 5 postimmunization, while during transfer EAE, positivity was revealed after 2 days postinjection of encephalitogenic lymphocytes. However, positivity for anti-P-selectin during preclinical EAE was present on fewer vessels than for the E-selectin mAb. No anti-P-selectin binding was detected during clinical EAE in either transfer or active models (Table III). Positivity for the anti-P-selectin mAb was not encountered even when the clinical score was 3 or 4 (data not shown). Alexa 488- or Alexa 566-labeled control Ab revealed no positivity during preclinical or clinical EAE (Fig. 8; data not shown). To obtain accurate results, in some experiments during the preclinical phase of EAE, we injected both Alexa 488-labeled anti-E-selectin mAb and Alexa 566 control mAb (data not shown). Interestingly, our experimental setting allowed us to observe that anti-selectin mAb binding had a patchy distribution and often positivity was encountered at sites where vessels branch, suggesting the existence of preferential recruitment areas.

Firm arrest of encephalitogenic lymphocytes requires rapid G_i-linked signaling

It is widely accepted that integrins require activation to promote rapid arrest under flow. It was previously shown that both LFA-1 and VLA-4 can mediate firm arrest after G_i-linked signaling to trigger activation of these integrins (24, 36, 37). We hypothesized that lymphocyte sticking in inflamed cerebral vessels may also involve PTX-sensitive signaling events. PTX treatment of autoreactive lymphocytes had no effect on rolling, but abolished 80% of the sticking fraction (Fig. 9). In contrast, a mutant holotoxin (PTX9K/129G) had no effect on arrest in brain vessels (24, 36, 38).

To assess a potential role of G_i-linked signaling in increasing the strength of adhesive interactions and, thus, slowing rolling and preparing the cell for full arrest, we also measured the V_{roll} of autoreactive lymphocytes in which $G_{\alpha i}$ proteins were blocked by PTX. There was no significant difference between V_{roll} of control lymphocytes and cells treated with PTX or mutant toxin (Table II; data not shown).

Discussion

The interaction between lymphocytes and brain endothelium is a central pathogenetic event in CNS autoimmunity and, thus, represents an important focus of investigation. In all previous brain intravital microscopy studies a cranial window into the skull was performed, which required respiratory assistance and was complicated by alterations of intracranial pressure, hemorrhage, and overheating of the brain surface secondary to drill and cautery use. To overcome these limitations, we developed a new model of in situ intravital microscopy in brain microcirculation that leaves the skull intact and maintains physiological intracranial pressure.

In our experiments, we adopted two sets of lymphocytes: PLN cells and brain-specific lymphocytes. We found that an inflamed brain endothelium, but not a nonactivated endothelium is able to mediate adhesion of lymphocytes; thus, we concluded that in our experimental model, the endothelium requires in vivo activation to support adhesive events. In inflamed cerebral vessels, we observed

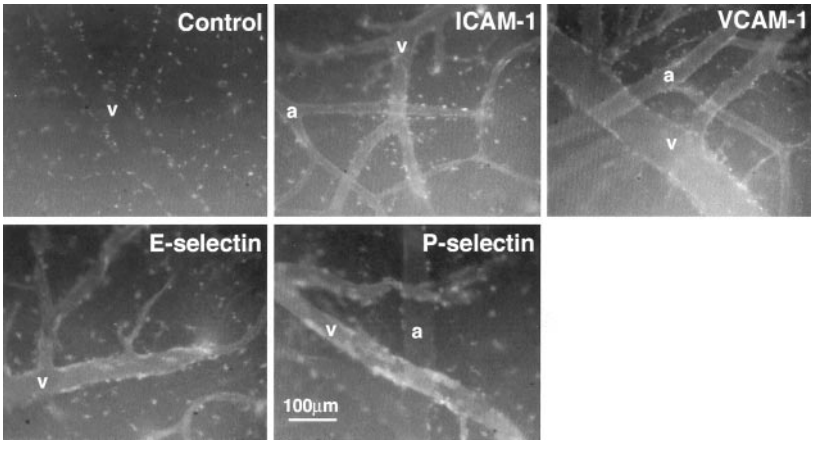

FIGURE 7. Expression of adhesion molecules in cerebral vessels after treatment of mice with LPS. Mice received 50 μg of Alexa 488-labeled mAb i.v. An isotype-matched Ab was used as control (see *Materials and Methods*). Both venules and arterioles were positive for VCAM-1 and ICAM-1, but only venules expressed endothelial selectins. *a* represents an artery, while *v* represents a venule. In the micrograph of P-selectin expression, the artery (*a*) is negative for P-selectin while the venule (*v*) is positive. Note that endothelial selectins have a less homogeneous distribution than ICAM-1 and VCAM-1.

Table III. *Expression of E- and P-selectin after LPS treatment and during EAE*[a]

	Hours/Days Postchallenge							
	0 h	2 h	5 h	1 day	2 days	5 days	6 days	9 days
LPS								
P-selectin	−	ND	+					
E-selectin	−	ND	+					
Active EAE								
P-selectin	−	ND	ND	ND	ND	+ (*)	−	−
E-selectin	−	ND	ND	ND	ND	+ (**)	+ (*)	+ (*) (disease)
Transfer EAE								
P-selectin	−	−	ND	−	+ (*)	−	ND	ND
E-selectin	−	−	ND	ND	+ (**)	+ (*) (disease)		

[a] Active and transfer EAE were induced as described in *Materials and Methods.* +, Vessels were positive for E- or P-selectin. E- and P-selectin were expressed by all examined venules in LPS-treated mice (12 μg/mouse). (**), Only patchy distribution with many vessels presenting positivity. (*), Only patchy distribution with very few vessels expressing positivity for the mAb. −, No positivity was observed. ND, not determined. Two mice per timepoint were used. Active EAE disease appeared on day 9 (all animals studied had a score of 2), while transfer EAE disease appeared on day 5 (animals had a score of 3 and of 2 for the E-selectin study, while mice in which we determined the positivity for P-selectin had a score of 2).

a low frequency of adhesive interactions using PLN cells (the majority naive), whereas Ag-specific lymphocytes efficiently interacted with the endothelium. Thus, efficient lymphocyte recruitment to brain microcirculation requires endothelium, as well as lymphocyte, preactivation. Rolling fractions of autoreactive lymphocytes were higher in vessels with small and medium calibers, but did not correlate with hemodynamic parameters such as mean blood flow velocity and wall shear stress, providing evidence that endothelial, but not hemodynamic, differences are responsible for lymphocyte rolling in mouse brain venules (23).

P- and E-selectin on endothelial cells are primary adhesion molecules for capture and the initiation of slow inflammatory rolling (39, 40). We showed that both P- and E-selectin are expressed on the brain endothelium after in vivo activation with LPS or TNF. In contrast to other intravital microscopy studies in other organs, where either E- or P-selectin are alone able to support leukocyte rolling, participation of both E- and P-selectin is required for efficient tethering and rolling in brain venules. Our data are in accordance with recent results showing that granulocytes also need both endothelial selectins to roll in cerebral vessels (17). We found that anti-PSGL-1 Abs, block 96% of capture and rolling in inflamed brain vessels, suggesting that PSGL-1 represents a key molecule in the tethering and rolling of lymphocytes in inflamed brain vessels. Moreover, recent results obtained by Carrithers et al. (18), suggested that P-selectin, a PSGL-1 ligand, may be involved in the early recruitment of encephalitogenic lymphocytes into the brain. Our results are also consistent with recent data showing that PSGL-1 is able to efficiently mediate tethering and rolling in vivo on both P- and E-selectins (41). Abs to PSGL-1 inhibit interactions of leukocytes to areas of inflammation in animal models (42, 43). Moreover, recombinant soluble forms of PSGL-1 inhibit selectin-mediated inflammatory responses in models of inflammation and thrombosis in vivo (44, 45). Taken together, these results suggest that inhibition of PSGL-1 interactions with endothelial selectins might prevent the accumulation of activated lymphocytes into the brain, having a protective role in autoimmune inflammatory diseases of the CNS. This is also supported by previous studies showing that sulfated polysaccharides are able to inhibit EAE presumably by interfering with the passage of lymphocytes across the brain endothelium (46, 47).

In our experimental model rolling interactions are also partially blocked by Abs to LFA-1 and VLA-4, suggesting that selectins and integrins must cooperate to ensure an efficient rolling. We found that Abs to these integrins or to ICAM-1 and VCAM-1 do not increase rolling velocity, suggesting that residual PSGL-1/endothelial selectin interactions are "per se" sufficient to mediate slow rolling. As shown for anti-integrin Abs, rolling velocity is not increased by PTX pretreatment, thus G_i-protein-linked signaling is not relevant for the strength of rolling interactions. However, it was previously shown under in vitro flow conditions that VLA-4 integrin-mediated rolling requires G_i-protein-linked signaling (37). The lack of involvement of integrins and G_i-protein-linked signaling in rolling velocity in our model could suggest that Ag-activated lymphocytes may have a significant proportion of integrins already organized in clusters, which is critical to integrin-dependent rolling (48). Notably, preliminary confocal microscopy data have revealed that the autoreactive lymphocytes that we used for our study already have LFA-1 and VLA-4 organized into big clusters (M. Majeed and G. Constantin, unpublished observation). Although integrins mediate part of the rolling, their engagement does not compensate for the inhibition induced by anti-PSGL-1 Abs, which block 96% of capture and rolling of autoreactive lymphocytes. Thus, we hypothesize that PSGL-1, but not integrins, is the critical molecule that mediates activated lymphocyte tethering on the inflamed brain endothelium.

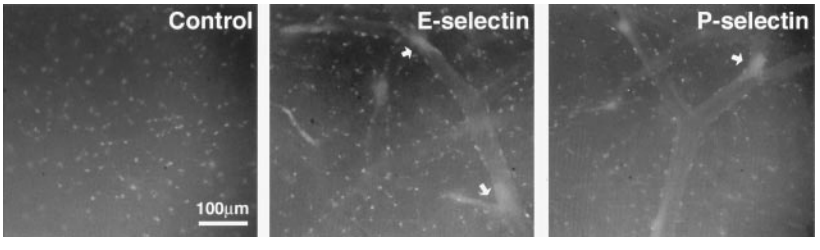

FIGURE 8. Alexa 488-labeled anti-E- and P-selectin and control mAb accumulation in cerebral vessels during preclinical phase of actively-induced EAE (day 5). Disease was induced in SJL mice as described in *Materials and Methods*. Note the patchy distribution of Ab positivity (arrows).

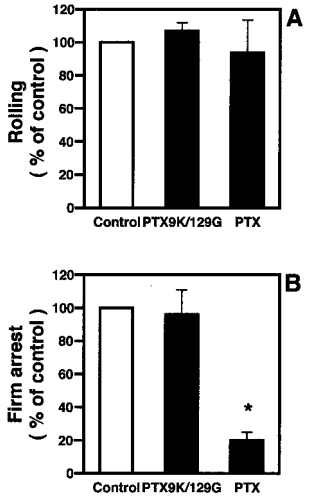

FIGURE 9. Arrest of autoreactive lymphocytes is blocked by PTX. Lymphocytes were Ag-stimulated for 4 days and then kept for 1–5 days in Ag-free medium before intravital microscopy experiments. Cells were treated for 2 h with 150ng/ml PTX or an inactive mutant form, PTX9K/129G. Rolling (*A*) and arrest (*B*) fractions of control and treated cells in cerebral venules was determined. Thirteen venules and five animals were examined (at least 1800 cells/condition). Data are expressed as mean ± SD. *, $p < 0.001$.

We documented positivity for both P- and E-selectin before the onset of EAE. Only E-selectin was expressed during clinical EAE. This was also previously found in vessels from acute plaques in MS patients (49). In contrast to our study, previous work by Engelhardt et al. (50) has shown that E- and P-selectin could not be up-regulated on the brain endothelium after LPS or TNF treatment of mice or during EAE. This discrepancy may be due to the fact that we used different mAbs and a more sensitive detection method of fluorescent videomicroscopy. It was previously shown that P-selectin is constitutively absent from cultured brain endothelial cells, but is up-regulated after 4 h of TNF or IL-1 stimulation (51). These data support our findings that a cytokine-activated, but not a normal, brain endothelium is able to express P-selectin. Our results are also in agreement with previous intravital microscopy studies in brain microcirculation showing a critical role of P- and E-selectin in granulocyte recruitment after activation of the endothelium (16, 17). It was previously shown that E- and P-selectin expression on the endothelium preferentially recruits Th1 cells (52). Thus, it is possible that during the preclinical phase of EAE, Th1, but not Th2, cells may be recruited. Further studies are required to clarify this issue. We also provide evidence that during the preclinical phase of EAE, potential "recruitment areas" that express endothelial selectins are up-regulated. These areas were often seen where vessels branch. Thus, as also shown by the exclusive expression of selectins on venules after in vivo LPS treatment, lower shear stress may favor the up-regulation of selectins on the brain endothelium. The presence of these recruitment areas may be of crucial importance to lymphocyte entry into the CNS and might explain the disposition in plaques of inflammation in MS patients.

LFA-1 and ICAM-1 were critical for lymphocyte sticking, whereas α_4 integrins and VCAM-1 have a lesser role, suggesting that during early inflammation in brain microvessels, LFA-1 and ICAM-1 are mainly responsible for firm arrest (Fig. 10). Moreover, we found that integrin-dependent firm arrest in brain microcirculation is blocked by PTX. Thus, as previously shown in studies on naive lymphocytes homing to Peyer's patches and lymph nodes (24, 36), Ag-specific lymphocytes also require in situ activation by an adhesion-triggering agonist which exerts its effect via a G_i-coupled surface receptor. This is the first demonstration showing the in vivo requirement for lymphocyte adhesion of a G_i-protein-linked signaling pathway in brain vessels. Notably, chemokines, which play a central role in lymphocyte adhesion triggering in secondary lymphoid organs, have been recently shown to trigger rapid LFA-1-dependent lymphocyte adhesion by inducing a high-affinity state and heterodimer lateral mobility leading to massive clustering (53). Interestingly, autoreactive lymphocytes already have a pool of LFA-1 and VLA-4 organized in clusters (M. Majeed and G. Constantin, unpublished observation). As stated above, this could be sufficient to mediate rolling, but not firm adhesion, as the inhibitory effect of PTX suggests, leading us to speculate that, as also suggested in Peyer's patches, integrin affinity triggering by locally presented chemokines may be required for rapid autoreactive lymphocyte arrest on cerebral vessels.

In conclusion, our results assign a critical role to PSGL-1/P-E-selectins and heterotrimeric G_i-linked signal transduction pathways as lymphocyte-endothelial determinants that control the adhesion in inflamed brain vessels. Our new approach to study brain microcirculation may provide a useful tool for further investigations of physiologic and pathologic events that occur in the CNS and may provide important information on the molecular mechanisms of leukocyte recruitment into the brain during inflammatory diseases.

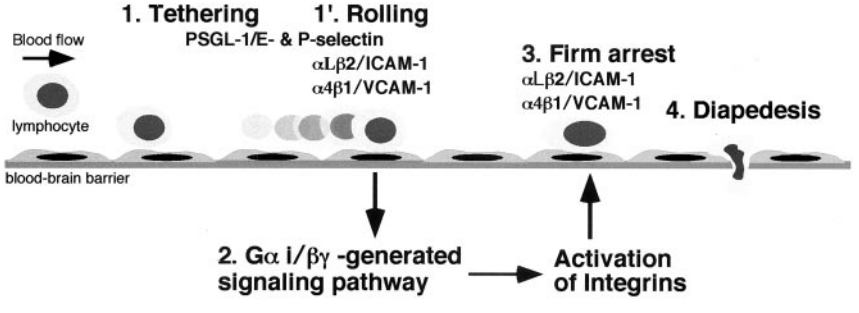

FIGURE 10. Recruitment of autoreactive lymphocytes in inflamed brain microcirculation is mediated by adhesion molecules and G_i-linked receptors. Three distinct steps were identified for autoreactive lymphocyte recruitment into the CNS: 1) expression of high levels of PSGL-1 on lymphocytes and up-regulation of endothelial selectins on the endothelium are critical for tethering and rolling; α_4 and $\alpha_L\beta_2$ integrins contribute to rolling but are not relevant for capture; 2) cells must encounter an activating factor expressed by the endothelium which triggers integrin activation through G_i protein-dependent signaling; and 3) integrin activation-dependent arrest is mediated mainly by LFA-1/ICAM-1 and by a lesser contribution from α_4 integrins/VCAM-1. Only cells that express high levels of PSGL-1 (naive cells that express lower levels of PSGL-1 are not able to efficiently interact with activated brain endothelium), high levels of LFA-1 and/or VLA-4, and the corresponding receptor(s) for the activating factor(s) presented by the endothelium will be able to efficiently be recruited in inflamed cerebral vessels.

References

1. Pettinelli, C. B., and D. E. McFarlin. 1981. Adoptive transfer of experimental allergic encephalomyelitis in SJL/J mice after in vitro activation of lymph node cells by myelin basic protein: requirement for Lyt 1^+ 2^- T lymphocytes. *J. Immunol. 127:1420.*
2. Lassmann, H., and K. Vass. 1996. Are current immunological concepts of multiple sclerosis reflected by the immunopathology of its lesions? In *Immunoneurology.* M. Chofflon and L. Steinman, eds. Springer-Verlag, Heidelberg, p. 77.
3. Hafle, D. A. 1999. The distinction blurs between an autoimmune versus microbial hypothesis in multiple sclerosis. *J. Clin. Invest. 104:527.*
4. Katz-Levy, Y., K. L. Neville, A. M. Girvin, C. L. Vanderlugt, J. G. Pope, L. J. Tan, and S. D. Miller. 1999. Endogenous presentation of self myelin epitopes by CNS-resident APCs in Theiler's virus-infected mice. *J. Clin Invest. 104:599.*
5. Butcher, E. C. 1991. Leukocyte-endothelial cell recognition: three (or more) steps to specificity and diversity. *Cell 67:1033.*
6. Springer, T. A. 1994. Traffic signals for lymphoid recirculation and leukocyte emigration: the multi-step paradigm. *Cell 76:301.*
7. Butcher, E. C., M. Williams, K. Youngman, L. Rott, and M. Briskin. 1999. Lymphocyte trafficking and regional immunity. *Adv. Immunol. 72:209.*
8. Butcher, E. C., and L. J. Picker. 1996. Lymphocyte homing and homeostasis. *Science 272:60.*
9. Hickey, W. F., B. L. Hsu, and H. Kimura. 1991. T-lymphocyte entry into the central nervous system. *J. Neurosci. Res. 28:254.*
10. Selmaj, K. 1996. Pathophysiology of the blood-brain-barrier. In *Immunoneurology.* M. Chofflon and L. Steinman, eds. Springer-Verlag, Heidelberg, p. 175.
11. Steffen, B. J., E. C. Butcher, and B. Engelhardt. 1994. Evidence for involvement of ICAM-1 and VCAM-1 in lymphocyte interaction with endothelium in experimental autoimmune encephalomyelitis in the central nervous system in the SJL/J mouse. *Am. J. Pathol. 145:189.*
12. Yednock, T., C. Cannon, L. C. Fritz, F. Sanchez-Madrid, L. Steinman, and N. Karin. 1992. Prevention of experimental autoimmune encephalomyelitis by antibodies against $\alpha_4\beta_1$ integrin. *Nature 356:63.*
13. Baron, J. L., J. A. Madri, N. H. Ruddle, G. Hashim, and C.A. Janeway, Jr. 1993. Surface expression of α_4 integrin by CD4 T cells is required for their entry into the brain parenchyma. *J. Exp. Med. 177:57.*
14. Gordon, E. J., K. J. Myers, J. P. Dougherty, H. Rosen, and Y. J. Ron. 1995. Both anti-CD11a (LFA-1) and anti-CD11b (MAC-1) therapy delay the onset and diminish the severity of experimental autoimmune encephalomyelitis. *J. Neuroimmunol. 62:153.*
15. Brocke, S., C. Piercy, L. Steinman, I. L. Weissman, and T. Veromaa. 1999. Antibodies to CD44 and integrin α_4, but not L-selectin, prevent central nervous system inflammation and experimental encephalomyelitis by blocking secondary leukocyte recruitment. *Proc. Natl. Acad. Sci. USA 96:6896.*
16. Yong, T., M. Q. Zheng, and D. S. Linthicum. 1997. Nicotine induces leukocyte rolling and adhesion in the cerebral microcirculation of the mouse. *J. Neuroimmunol. 80:158.*
17. Carvalho-Tavares, J., M. J. Hickey, J. Hutchison, J. Michaud, I. T. Sutcliffe, and P. Kubes. 2000. A role for platelets and endothelial selectins in TNFα-induced leukocyte recruitment in the brain microvasculature. *Circ. Res. 87:1141.*
18. Carrithers, M. D., I. Visintin, S. K. Kang, and C.A. Janeway, Jr. 2000. Differential adhesion molecule requirements for immune surveillance and inflammatory recruitment. *Brain 123:1092.*
19. Walter, U. M., L. M. Ayer, A. M. Manning, P. S. Frenette, D. D. Wagner, R. O. Hynes, B. A. Wolitzky, and A. C. Issekutz. 1997. Generation and characterization of a novel adhesion function blocking monoclonal antibody recognizing both rat and mouse E-selectin. *Hybridoma 16:355.*
20. Walter, U. M., L. M. Ayer, B. A. Wolitzky, D. D. Wagner, R. O. Hynes, A. M. Manning, and A. C. Issekutz. 1997. Characterization of a novel adhesion function blocking monoclonal antibody to rat/mouse P-selectin generated in the P-selectin-deficient mouse. *Hybridoma 16:249.*
21. Frenette, P., C. V. Denis, L. Weiss, K. Jurk, S. Subbarao, B. Kehrel, J. H. Hartwig, D. Vestweber, and D. D. Wagner. 2000. P-selectin glycoprotein ligand-1 (PSGL-1) is expressed on platelets and can mediate platelet-endothelial interactions in vivo. *J. Exp. Med. 191:1413.*
22. Constantin, G., C. Laudanna, S. Brocke, and E. Butcher. 1999. Inhibition of experimental autoimmune encephalomyelitis by a tyrosine kinase inhibitor. *J. Immunol. 162:1144.*
23. Ley, K., and P. Gaehtgens. 1991. Endothelial, not hemodynamic, differences are responsible for preferential leukocyte rolling in rat mesenteric venules. *Circ. Res. 69:1034.*
24. Warnock, R. A., S. Askari, E. C. Butcher, and U. H. von Andrian. 1998. Molecular mechanisms of lymphocyte homing to peripheral lymph nodes. *J. Exp. Med.* 187:205.
25. Constantin, G., S. Brocke, A. Izikson, C. Laudanna, and E. Butcher. 1998. Tyrphostin AG490, a tyrosine kinase inhibitor, blocks actively-induced experimental allergic encephalomyelitis. *Eur. J. Immunol. 28:3523.*
26. Scremin, O. U. 1995. Cerebral vascular system. In *The Rat Nervous System.* G. Paxinos, ed. Academic Press, New York, p. 3.
27. Mazo, I. B., J. C. Gutierrez-Ramos, P. S. Frenette, R. O. Hynes, D. D. Wagner, and U.H. von Andrian. Hematopoietic progenitor cell rolling in bone marrow microvessels: parallel contributions by endothelial selectins and vascular cell adhesion molecule 1. *J. Exp. Med. 188:465.*
28. Henninger, D. D., J. Panes, M. Eppihimer, J. Russel, M. Gerritsen, D. C. Anderson, and D. N. Granger. 1997. Cytokine-induced VCAM-1 and ICAM-1 expression in different organs of the mouse. *J. Immunol. 158:1825.*
29. Gotsch, U., U. Jager, M. Dominis, and D. Vestweber. 1994. Expression of P-selectin on endothelial cells is upregulated by LPS and TNF-α in vivo. *Cell. Adhes. Commun. 2:7.*
30. Henseleit, U., K. Steinbrink, M. Goebeler, J. Roth, D. Vestweber, C. Sorg, and C. Sunderkotter. 1996. E-selectin expression in experimental models of inflammation in mice. *J. Pathol. 180:317.*
31. Berlin, C., R. F. Bargatze, J. J. Campbell, U.H. von Andrian, M. C. Szabo, S. R. Hassler, R. D. Nelson, E. L. Berg, and E. C. Butcher. 1995. α_4 integrins mediate lymphocyte attachment and rolling under flow. *Cell 80:413.*
32. Johnston, B., T. B. Issekutz, and P. Kubes. 1996. The α_4-integrin supports leukocyte rolling and adhesion in chronically inflamed postcapillary venules in vivo. *J. Exp. Med. 183:1995.*
33. Henderson, R. B., L. H. K. Lim, P. A. Tessier, F. N. E. Gavins, M. Mathies, M. Peretti, and N. Hogg. 2001. The use of lymphocyte function-associated antigen (LFA)-1-deficient mice to determine the role of LFA-1, Mac-1, and α_4 integrin in the inflammatory response of neutrophils. *J. Exp. Med. 194:219.*
34. Bargatze, R. F., M. A. Jutila, and E. C. Butcher. 1995. Distinct roles of L-selectin and integrins $\alpha_4\beta_7$ and LFA-1 in lymphocyte homing to Peyer's patch-HEV in situ: the multistep model confirmed and refined. *Immunity 3:99.*
35. Jung, U., K. E. Norman, K. Scharffetter-Kochanek, A. L. Beaudet, and K. Ley. 1998. Transit time of leukocytes rolling through venules controls cytokine-induced inflammatory cell recruitment in vivo. *J. Clin. Invest. 102:1526.*
36. Bargatze, R. F., and E. C. Butcher. 1993. Rapid G protein-regulated activation event involved in lymphocyte binding to high endothelial venules. *J. Exp. Med. 178:367.*
37. Chan, J. R., S. J. Hyduk, and M. I. Cybulsky. 2001. Chemoattractants induce a rapid and transient upregulation of monocyte α_4 integrin affinity for vascular cell adhesion molecule 1 which mediates arrest: an early step in the process of emigration. *J. Exp. Med. 193:1149.*
38. Pizza, M., A. Covacci, A. Bartoloni, M. Perugini, L. Nencioni, M. T. De Magistris, L. Villa, D. Nucci, R. Manetti, M. Bugnoli, et al. 1989. Mutants of pertussis toxin suitable for vaccine development. *Science 246:497.*
39. Johnston, B., U. M. Walter, A. C. Issekutz, T. B. Issekutz, D. C. Anderson, and P. Kubes. 1997. Differential roles of selectins and the α_4-integrin in acute, subacute, and chronic leukocyte recruitment in vivo. *J. Immunol. 159:4514.*
40. Ley, K., M. Allietta, D. C. Bullard, and S. Morgan. 1998. Importance of E-selectin for firm leukocyte adhesion in vivo. *Circ. Res. 83:287.*
41. Norman, K. E., A. G. Katopodis, G. Thoma, F. Kolbinger, A. E. Hicks, M. J. Cotter, A. G. Pockley, and P. G. Hellewell. 2000. P-selectin glycoprotein ligand-1 supports rolling on E- and P-selectin in vivo. *Blood 96:3585.*
42. Borges, E., R. Eytner, T. Moll, M. Steegmaier, M. A. Campbell, K. Ley, H. Mossmann, and D. Vestweber. 1997. The P-selectin glycoprotein ligand-1 is important for recruitment of neutrophils into inflamed mouse peritoneum. *Blood 90:1934.*
43. Borges, E., W. Tietz, M. Steegmaier, T. Moll, R. Hallmann, A. Hamann, and D. Vestweber. 1997. P-selectin glycoprotein ligand-1 (PSGL-1) on T helper 1 but not on T helper 2 cells binds to P-selectin and supports migration into inflamed skin. *J. Exp. Med. 185:573.*
44. Kumar, A., M. P. Villani, U. K. Patel, J.C. Keith, Jr., and R. G. Schaub. 1999. Recombinant soluble form of PSGL-1 accelerates thrombolysis and prevents reocclusion in a porcine model. *Circulation 99:1363.*
45. Scalia, R., V. E. Armstead, A. G. Minchenko, and A. M. Lefer. 1999. Essential role of P-selectin in the initiation of the inflammatory response induced by hemorrhage and reinfusion. *J. Exp. Med. 189:931.*
46. Willenborg, D. O., and C. R. Parish. 1988. Inhibition of allergic encephalomyelitis in rats by treatment with sulfated polysaccharides. *J. Immunol. 140:3401.*
47. Willenborg, D. O., C. R. Parish, and W. B. Cowden. 1989. Phosphosugars are potent inhibitors of central nervous system inflammation. *FASEB J. 3:1968.*
48. Grabovsky, V., S. Feigelson, C. Chen, D. A. Bleijs, A. Peled, G. Cinamon, F. Baleux, F. Arenzana-Seisdedos, T. Lapidot, Y. van Kooyk, et al. 2000. Subsecond induction of α_4 integrin clustering by immobilized chemokines stimulates leukocyte tethering and rolling on endothelial vascular cell adhesion molecule 1 under flow conditions. *J. Exp. Med. 192:495.*
49. Lee, S. J., and E. N. Benveniste. 1999. Adhesion molecule expression and regulation on cells of the central nervous system. *J. Neuroimmunol. 98:77.*
50. Engelhardt, B., D. Vestweber, R. Hallmann, and M. Schulz. 1997. E- and P-selectin are not involved in the recruitment of inflammatory cells across the blood-brain barrier in experimental autoimmune encephalomyelitis. *Blood 90:4459.*
51. Barkalow, F., M. Goodman, M. Gerritsen, and T. N. Mayadas. 1996. Brain endothelium lack one of two pathways of P-selectin-mediated neutrophil adhesion. *Blood 88:4585.*
52. Austrup, F., D. Vestweber, E. Borges, M. Lohhning, R. Bauer, U. Herz, H. Renz, R. Hallmann, A. Scheffold, A. Radbruch, and A. Hamann. 1997. P- and E-selectin mediate recruitment of T-helper-1 but not T-helper-2 cells into inflamed tissues. *Nature 385:81.*
53. Constantin, G., M. Majeed, C. Giagulli, L. Piccio, J. Y. Kim, and C. Laudanna. 2000. Chemokines trigger immediate β_2 integrin affinity and mobility changes: differential regulation and roles in lymphocyte arrest under flow. *Immunity 16:759.*